



Thermal Stability and Aging Characteristics of HNBR/Clay Nanocomposites in Air, Water and Oil at Elevated Temperature

Huang Anmin¹, Wang Xiaoping^{1*}, Jia Demin¹, Li Yanmei²

¹ Department of Polymer Materials and Engineering, South China University of Technology, Guangzhou, Guangdong 510640, P R China; fax: +86-20-2223-6688; wangxp@scut.edu.cn

² Schlumberger, Rosharon, Texas 77583, USA; yli@rosharon.oilfield.slb.com.

(Received: 5 March, 2007; published: 16 May, 2007)

Abstract: Hydrogenated nitrile rubber (HNBR)/clay nanocomposites are prepared using conventional two-roll mill mixing technique. The structure and morphology of nanocomposites are characterized using wide angle X-ray diffraction (WAXD) and transmission electron microscopy (TEM). Both intercalated and exfoliated clay structures are observed in HNBR/clay nanocomposites. The thermal stability of the nanocomposites is studied using thermogravimetric analysis (TGA) and TGA-Fourier transform infrared (FTIR) spectroscopy. The effect of organoclay on physical and mechanical properties of HNBR vulcanizates before and after aging in air, water and oil at 178 °C is also investigated. It is found that adding organoclay in HNBR elastomer greatly improves material thermal stability and aging performance in different medium at elevated temperature.

Key words: Hydrogenated nitrile rubber; Organoclay; Nanocomposites; Thermal stability; Aging; Water resistance; Oil resistance;

Introduction

Organic/inorganic hybrid nanocomposites have great potentials for novel material applications because distinct material properties from both organic and inorganic components can be combined in a material with uniform mixing at the nano-scale. Furthermore, synergistic improvements in properties are often observed in the nanocomposites. Elastomer/layered silicate nanocomposites have drawn great attentions from both academic and industrial researchers because these nanocomposites often exhibit dramatically enhanced physical and/or chemical properties even with small amount of nano-filler in comparison with conventional microscale composites [1–9]. It is believed that the superior properties of the elastomer/clay nanocomposites come not only from nano-scale dispersion of clay particles in the elastomer matrix but also from the strong interactions between the elastomer matrix and the clay layers [10–18]. To improve this interaction, various cationic surfactants with functional groups have been used to modify the clay through an ion-exchange reaction. Clay can also provide excellent barrier properties [19–21], form multicellular char residue [22, 23] and lower the molecular mobility of polymer [24] when dispersed uniformly at nano-scale and incorporated well with polymer matrix; these factors are contributing to the increased thermal stability of the nanocomposites.

Hydrogenated nitrile rubber (HNBR) was introduced in the early 1980's by Bayer as a new material for permanent exposure to temperatures between -25 °C and 150 °C.

HNBR received special attention because its saturated backbone with highly polar acrylonitrile groups has good heat, oil, ozone, and chemical resistance even under adverse conditions. HNBR vulcanizates can be reinforced by conventional fillers as other synthetic elastomers [25-27]. With rapid advancement of nano-technology in rubber industry, organoclay and other nano fillers are introduced to HNBR elastomers as a new filler system [12, 13]. This technology leads to high performance HNBR elastomers to meet the increasing demand of automotive, aerospace and other industries for extremely high operating temperatures and extended material service lifetime. However, there is not much study carried out on how organoclay fillers affect HNBR thermal stability and aging performance under severe conditions. Therefore, the focus of this research study is to investigate if adding organoclay can help improve thermal stability and air-water-oil resistance of HNBR elastomer at extremely high temperatures. If it does, then what is the working mechanism and to obtain a better understanding of the full picture, various characterization and testing techniques including WAXD, TEM, TGA and TGA-FTIR are utilized throughout this study.

Results and discussion

Structure and morphology of HNBR/clay nanocomposites

Wide angle X-ray diffraction (WAXD) is a conventional technique to determine the interlayer spacing of clay particles inside polymer/clay nanocomposites. Figure 1 shows WAXD patterns for the original clay, modified clay, plain HNBR vulcanizate, HNBR/clay compound before curing and HNBR/clay vulcanizates with different clay content. Before modification, the interlayer spacing $d(001)$ of the original clay is 1.30 nm. After modification, the d -spacing is increased to 3.04 nm.

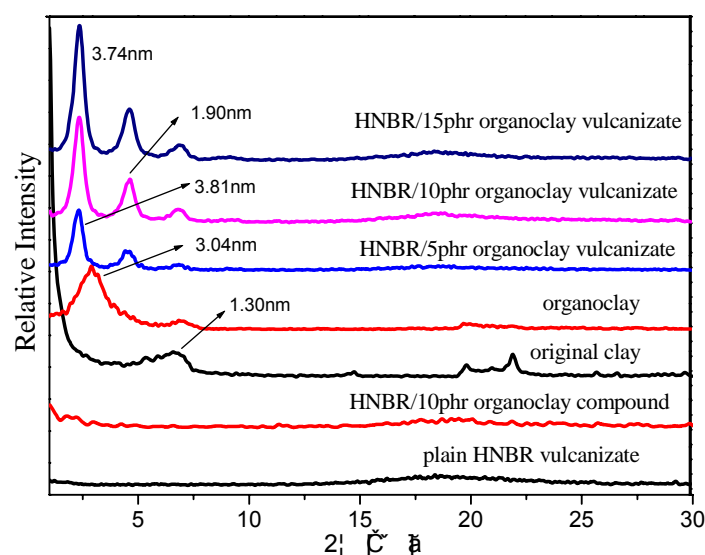


Fig. 1. WAXD patterns for different materials.

In HNBR/clay vulcanizates, the d -spacing of clay is further increased from 3.04 nm to 3.74~3.81 nm. This indicates a good interaction between organoclay and the HNBR rubber matrix, which helps expand clay interlayer spacing as well as dispersion of clay particles. Similar findings were made by other researchers in different material systems [28-30]. Other than the peak observed around d -spacing of 3.74~3.81 nm in

HNBR/clay nanocomposites, two smaller peaks are also observed around d-spacing of 1.9 nm and 1.3 nm. One reflection peak with a basal spacing of 1.3 nm suggests some of the clay particles still maintain their original interlayer spacing. The spacing of other one is 1.9 nm, which is less than that for organoclay but much larger than that of original clay. The further collapsed structure is termed deintercalation (“extraction” of the intercalation) [15]. Clay concentration does not have much effect on the WAXD patterns in different HNBR/clay nanocomposites, but on the intensities of the peaks. WAXD peaks observed in HNBR/clay vulcanizates suggest the majority of clay particles are intercalated with HNBR matrix.

More interestingly, no WAXD peak is observed in HNBR/organoclay compound. This suggests exfoliated clay structure is formed in the compound during mixing. Later TEM study confirms this finding (Fig 2a). However, this exfoliated clay structure is not fully retained upon curing. Instead, intercalated clay structure is formed and becomes the dominant structure in the vulcanizates. The change of clay structure upon curing was also observed by other researchers [12, 31]. It is suggested that the processing conditions, such as pressure, temperature, and curing time, play important roles in determining final clay structure in cured products. Detail discussion on how these processing conditions affect clay structure in HNBR/clay nanocomposites in this study will be reported in a separate paper.

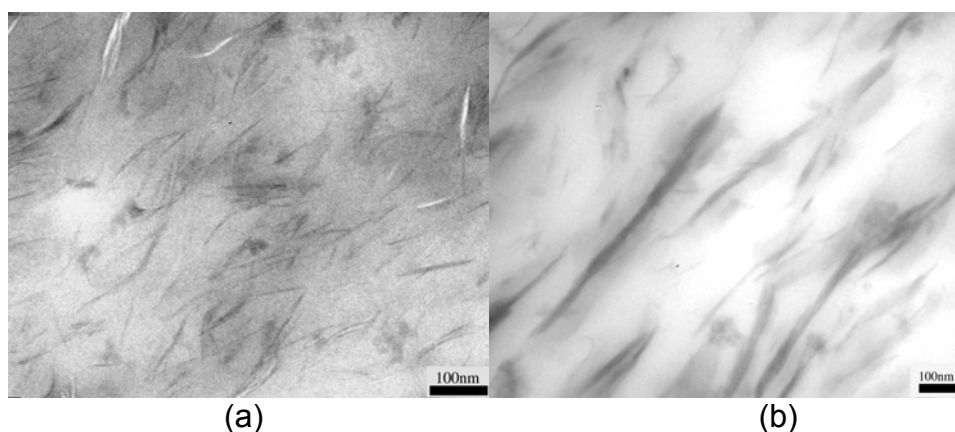


Fig. 2. TEM morphology of HNBR/organoclay compound (a) and vulcanizate (b).

Figure 2 shows TEM morphology of HNBR/clay nanocomposite before and after curing. The dark lines represent cross-section of individual clay layers which are about 1 nm thick. The gap between two adjacent layers is the interlayer spacing or gallery. Clay particles are fully exfoliated during mixing process (Fig 2a). However, intercalated clay structure is reformed during vulcanization as discussed in WAXD session. Organoclay bundles consisting of several clay layers are observed in the vulcanizate (Fig 2b). A few single clay layers are also observed adjacent to these bundles. The thickness of these organoclay bundles is usually smaller than 50 nm. Typical sandwich structure consisting of parallel alternating organoclay layers and HNBR matrix observed in this TEM photograph indicates the coexistence of intercalated/exfoliated clay structure [17, 32].

Mechanical and medium ageing properties

For comparison purpose, HNBR filled with 30 phr conventional carbon black is also studied along with HNBR/clay nanocomposites using the same base formula. From Table 1, it is found that similar mechanical properties can be achieved with small amount of clay (10 phr clay or more) compared with large amount of carbon black reinforcing system [2]. Modulus, tensile strength and elongation at break are increased with clay content, then levels off at 10 phr. A noticeable increase in permanent set with clay content is also observed. This may or may not be desirable depending on the application requirements.

Tab. 1. Physical and mechanical properties of different HNBR vulcanizates.

Organoclay (phr)		0	2.5	5	7.5	10	15
Carbon black (phr)	30						
Modulus at 100% elongation (MPa)	1.8	0.9	1.2	1.4	1.5	1.9	2.1
Shore A hardness	58	48	51	55	56	59	63
Tensile strength (MPa)	28.0	7.4	10.8	16.8	18.1	20.5	20.7
Elongation at break (%)	420	495	490	500	520	530	525
Permanent set (%)	12	8	10	14	18	24	36

The aging performance of HNBR/clay nanocomposites is studied at 178 °C in air, water and oil, respectively. It should be noted that the aging temperature used in this study exceeds recommended application temperature for HNBR elastomer from HNBR suppliers [27, 33]. One purpose of choosing this temperature is to accelerate aging process. The other purpose is to find out if HNBR/clay nanocomposites can perform better under these severe conditions. Table 2~4 summarize the change of material properties after aging in different media for extended hours. It is clear that adding organoclay significantly improves material performance at high temperature in both air and oil. HNBR/nanocomposites maintain about 80% of tensile strength after aging in air and 50% of tensile strength after aging in oil. However, HNBR reinforced with conventional carbon black loses most of its mechanical properties after aging in air and oil. Aging performance of HNBR nanocomposites in water is similar to that of carbon black filled HNBR. This may be due to the swelling of the material with the presence of organoclay, which counter-interacts with its reinforcing effect. It is also found that the retention of material properties is not affected much by clay content when it is greater than 2.5 phr.

Tab. 2. Material properties of HNBR vulcanizates after air aging at 178 °C for 96 hours.

Organoclay (phr)		0	2.5	5	7.5	10	15
Carbon black (phr)	30						
Change in hardness	+15	+4	+7	+7	+8	+8	+9
Tensile strength (MPa)	13.5	4.4	9.5	15.0	15.7	16.5	16.4
Retention of tensile strength (%)	48.2	58.8	88.0	89.3	86.7	80.8	79.2
Elongation at break (%)	130	230	300	375	370	380	370
Retention of elongation at break (%)	30.9	46.5	61.2	75.0	71.2	71.7	70.5
Permanent set (%)	6	2	8	12	14	16	36

Tab. 3. Material properties of HNBR vulcanizates after water aging at 178 °C for 96 hours.

Organoclay (phr) Carbon black (phr)	30	0	2.5	5	7.5	10	15
Change in hardness	+7	-1	+1	+1	+2	+2	+3
Tensile strength (MPa)	24.8	5.3	9.6	14.7	15.4	17.1	16.6
Retention of tensile strength (%)	88.6	71.6	88.9	87.5	84.9	83.6	80.4
Elongation at break (%)	360	470	545	540	530	520	515
Retention of elongation at break (%)	85.7	94.9	111.2	108.0	101.9	98.1	98.1
Permanent set (%)	8	8	16	18	20	24	40

Tab. 4. Material properties of HNBR vulcanizates after oil aging at 178 °C for 72 hours.

Organoclay (phr) Carbon black (phr)	30	0	2.5	5	7.5	10	15
Change in hardness	+19	-1	-2	+1	+3	+2	+1
Tensile strength (MPa)	7.4	3.8	5.5	8.6	10.6	12.1	11.0
Retention of tensile strength (%)	26.4	51.3	50.9	51.2	58.6	59.0	53.1
Elongation at break (%)	135	115	190	255	270	250	235
Retention of elongation at break (%)	32.1	23.2	38.8	50.8	51.9	47.2	44.8
Permanent set (%)	2	4	4	2	4	4	4
Change in mass (%)	12.6	16.5	14.4	13.1	12.9	12.3	11.2

Thermogravimetric analysis

To better understand how organoclay helps improve material performance at high temperature, an in-depth thermogravimetric study using TGA and TGA-FTIR is carried out on different materials.

-Thermal stability analysis

Thermal degradation analysis of HNBR vulcanizates is performed in both nitrogen and air atmosphere, respectively. The TGA curves of different HNBR vulcanizates in nitrogen (Fig.3a) exhibit one major degradation step around 733K, which is associated with the decomposition of polymer chain. This claim is confirmed with later TGA-FTIR results. However, the TGA curves in air (Fig. 3b) exhibit two major degradation steps around 738 K and 768 K respectively. For comparison purpose, temperatures at the maximum rate of decomposition for different materials in the derivative thermograms (DTG) are designated as T_p , and summarized in Table 5. It should be noted that T_p is higher in air than in nitrogen. This is caused by the faster heating rate in air.

From Table 5, it can be seen that T_p is greatly improved with the addition of organoclay, and it is increased with clay content. It is believed that layered clay particles can insulate underlying materials and provide tortuous path for heat/gas transportation [34]. This in turn, slows down the degradation process significantly.

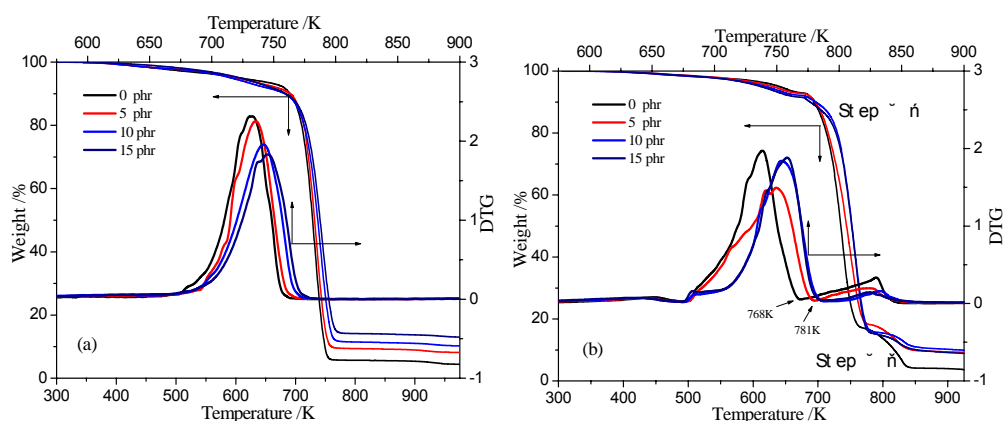


Fig. 3. TGA and DTG curves of HNBR vulcanizates with different clay content in (a) nitrogen (Heating rate, 10 K /min) and (b) air (Heating rate, 20 K /min)

Tab. 5. T_p of different HNBR vulcanizates in N_2 and air atmosphere.

Organoclay /phr	T_p in N_2 atmosphere /K	T_p of step I in air atmosphere / K	T_i^a of step II in air atmosphere / K
0	731	738	768
5	736	749	781
10	742	754	787
15	745	759	787

T_i^a : Starting decomposition temperature of step II in air atmosphere

A second degradation step observed at higher temperature in air suggests a different degradation mechanism [35]. It is suspected that $-CN$ group in the decomposition product from Step I can react with oxygen to form a more stable condensation product via condensation reaction. This condensation product then decomposes at a higher temperature in Step II. With the addition of organoclay, both T_p and T_i^a (starting degradation temperature) are increased significantly.

-Decomposition kinetics

Decomposition kinetics in filled and unfilled HNBR vulcanizates in nitrogen is studied using Ozawa's method [36, 37] and Kissinger's method [38] due to their simplicity. Ozawa's method is an integral method that is used to determine the activation energy, E_d , without knowledge of reaction order. Kissinger's method is a differential method. The activation energy can be calculated by assuming 1.0-order reaction without a precise knowledge of the reaction mechanism [39]. The slope and intercept of the plot at different heating rates (β) are used to calculate the activation energy E_d by the least squares method.

TGA curves are shifted to higher temperatures at faster heating rates. The shift derives from the basic kinetic formal equation: $d\alpha/dT = (1/\beta) (1-\alpha)^n$. At the same α , rate inversely depends on heating rate. Data at T_p are then used to generate plots of $\lg \beta$ or $\ln (\beta / T_p^2)$ against $(1/T_p)$ as shown in Figure 4. Table 6 summarizes the activation energy for filled and unfilled HNBR vulcanizates using both Ozawa's and Kissinger's equations. Two methods yield similar results. This suggests that the activation energy of HNBR vulcanizates can be obtained with either integral or differential method.

In Table 6, it can be seen that E_d is increased dramatically with clay content. It is improved about 35% in HNBR/15 phr organoclay vulcanizate compared with plain HNBR vulcanizate. The thermal stability of HNBR/clay nanocomposites is related to the nanocomposites' structure, organoclay content and the dispersion [40]. This trend is consistent with previous TGA study (Table 5).

The above finding further proves that adding organoclay help improve the thermal stability of HNBR vulcanizates to a significant degree.

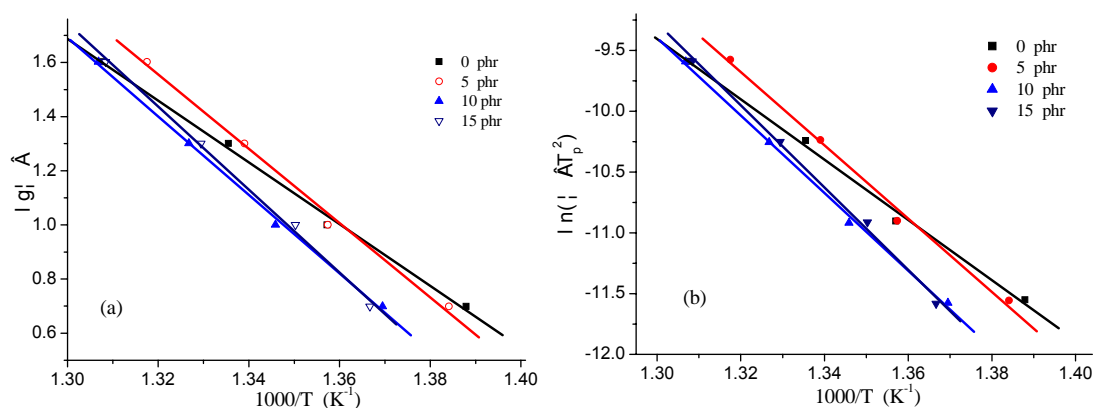


Fig. 4. Ozawa plots (a) and Kissinger plots (b) for different HNBR vulcanizates.

Tab. 6. Activation energy for different HNBR vulcanizates in nitrogen.

Organoclay /phr	E_d (KJ/mol)	
	Ozawa	Kissinger
0	207.5	206.1
5	250.0	250.5
10	264.2	265.3
15	279.1	281.1

-Degradation mechanism

To further understand how organoclay helps improve thermal stability of HNBR vulcanizates, a TGA-FTIR study is performed on both plain HNBR vulcanizate and HNBR filled with 10 phr organoclay particles. Figure 5 shows the in-situ FTIR spectra of degraded products from both materials at different degradation temperatures. The FTIR peaks at 2933 cm^{-1} , 2865 cm^{-1} , and 1459 cm^{-1} are assigned to alkyl groups ($-\text{CH}_2$, $-\text{CH}_3$). The peak at 2236 cm^{-1} is assigned to nitrile group ($-\text{CN}$), and the peak at 2361 cm^{-1} is assigned to the background gas CO_2 . No decomposition products are detected by FTIR when temperature is below 623 K. This may be due to fact that the concentration of the volatiles is too low or the decomposed products are not in the vapor state. It is shown in Figure 5 that the absorbance of plain HNBR vulcanizate is stronger than that of HNBR/10 phr organoclay vulcanizate. At temperature around 688 K, major degradation process is initiated in both materials indicated by the appearance of peaks for alkyl and nitrile groups. The intensity of these peaks reaches the maximum at about 733 K, and then decreases with degradation temperature. In plain HNBR vulcanizate, no nitrile group is detected beyond 873 K. This suggests HNBR vulcanizate is completely degraded. However, in organoclay filled HNBR vulcanizate, both alkyl and nitrile groups can still be detected as degraded products at 1013 K. This

further proves that organoclay can slow down the degradation process and greatly improve the thermal stability of HNBR vulcanizates.

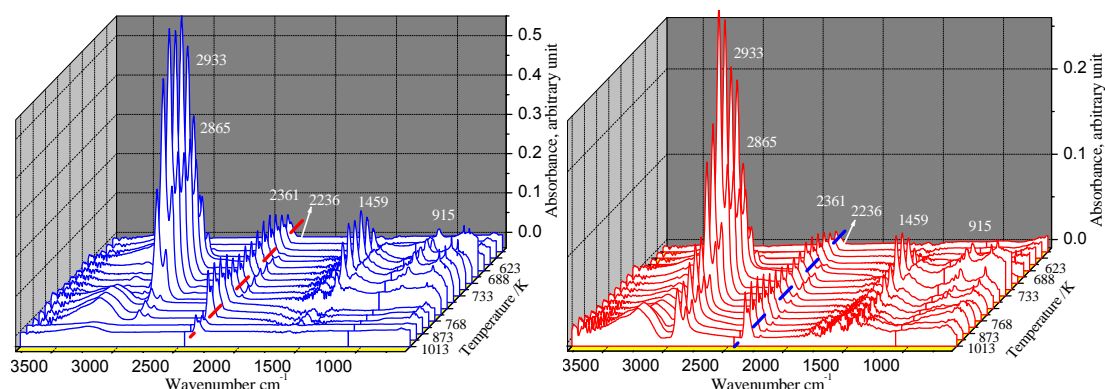


Fig. 5. FTIR spectra of decomposed products from TGA (in nitrogen atmosphere (@10 K /min heating rate) for unfilled HNBR vulcanizate (a) and HNBR/10 phr organoclay vulcanizate (b)

Based on the above findings, the following model/mechanism (Fig. 6) is proposed: Organoclay particles are exfoliated mostly during mixing process and dispersed uniformly and randomly in the rubber matrix. This comes from shear stress in mixing as well as the good interaction between the rubber matrix and the filler system. However, during the curing process, they are partially intercalated and orientated due to the heat, pressure and the tension force generated by crosslinking reaction. This results in co-existence of intercalated and exfoliated clay structures in HNBR nanocomposites.

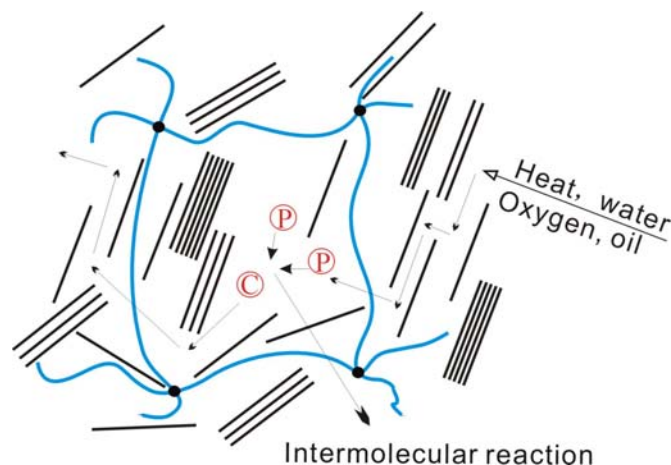






Fig. 6. Schematic illustration of HNBR/organoclay vulcanizates.  HNBR molecular chain,  crosslinking point,  decomposition product,  complex compounds.

The strong interfacial adhesion, clay orientation and intercalated-exfoliated clay structure are the key factors for enhanced mechanical properties. In HNBR/clay nanocomposites exposed to high temperature the organoclay layers provide effective barriers and tortuous path to heat, oxygen, water, and oil evolved, thus slowing down the rate of mass loss during thermal decomposition of HNBR/clay nanocomposites. Meanwhile, the barrier effect brings the superheated conditions in the condensed

phase. The long carbon-chain alkyl quaternary ammonium salts in organoclay and HNBR matrix are decomposed. New products in gaseous and condensed phase are formed following additional degradation pathways. Then chemical species, trapped between clay layers, have more opportunity to undergo further intermolecular reactions, such as radical recombination. The intermolecular reactions lead to the formation of complex compounds thus lowering the volatilization rate and favour the char formation process [41]. As a result, the thermal stability and aging properties in different medium of HNBR vulcanizates are improved significantly.

Conclusions

Both intercalated and exfoliated clay structures are observed in HNBR/clay nanocomposites. Similar mechanical properties can be achieved with small amount of organoclay (10 phr or more) compared with large amount of carbon black reinforcing system. Furthermore, HNBR vulcanizates reinforced with organoclay exhibit much better thermal stability and aging performance in air, water and oil. The increased thermal stability and aging properties may come from uniform dispersion of clay particles at nano-scale, good interaction between clay particles and HNBR matrix, and excellent barrier properties of organoclay particles.

Experimental part

Materials

HNBR having 36% acrylonitrile content was provided by Zeon Chemical, Japan. The Mooney viscosity ML (1+4) 100 °C of the rubber is 85. Montmorillonite (MMT) modified with dimethyltallow-dihydrogenated quaternary ammonium salt (Fig.6) was obtained from Southern Clay Inc, TX, USA. Other compounding ingredients were obtained from local suppliers.

The compounds were mixed on a two-roll mill (friction ratio 1:1.12) below 60 °C for 15 min. HNBR was first masticated for 2 min. After thorough plasticizing, accelerating agent, anti-ageing agent, activating agent, and clay were added in sequence. Curing agent dicumyl peroxide (DCP) was added at last. The optimum cure time (Tc90) was determined by U-CAN UR-2030 vulcameter, Taiwan. The samples for tensile testing were then prepared in an electrically heated press at 170°C for Tc90.

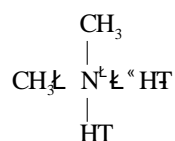


Fig. 6. Molecular structure of intercalating agent for MMT; HT: hydrogenated tallow group (~65% C₁₈; ~30% C₁₆; ~5% C₁₄).

Wide angle X-ray diffraction

A Ragaku Model D/MAX-β diffractometer was used to study WAXD pattern of clay and HNBR/clay nanocomposites. Testing was carried out with 2θ scanned between 1° and 30° at 1°/min scanning rate and 0.02 chopper increment, using Cu Kα (λ=0.15418 nm) radiation. Specimens with dimensions of 20×20×2 (length×width×thickness) mm³ were used.

Transmission electron microscopy

For the TEM sample preparation, specimens were carefully trimmed to an appropriate size ($10 \times 4 \text{ mm}^2$). Ultra-thin sections, ranging from 60 to 80 nm, were obtained using a Super Nova 655001 instrument (Leica, Switzerland) with a diamond knife at -150°C . The thin sections were placed on 200-mesh formvar-coated copper grids and examined using a TEM 2000 CM-300 instrument (Philip) operated at an accelerating voltage of 200 kV.

Thermal stability

The TGA and TGA-FTIR tests were performed using Netzsch TG 209F1 and TG 209, DE, respectively. Samples ($10.0 \pm 0.5 \text{ mg}$) were heated from ambient temperature to 700°C under nitrogen and air atmosphere, respectively, at a flow rate of 40 ml/min. TGA tests were carried out at four different heating rates (5, 10, 20, 40 K /min) for decomposition kinetics study.

Environmental ageing

Aging test in air was conducted following ISO standard 188-2003. Dumbbell specimens were placed in a circulating air oven at 178°C for 4 days. Ageing tests in water and oil were carried out following ISO standard 1817-1999. In water aging test, samples were placed in 10 L airtight reaction kettle at 178°C (0.9 MPa) for 4 days. In oil aging test, samples were immersed in automatic transmission fluid (ATF) at 178°C for 3 days.

Mechanical properties

Tensile tests were conducted on both non-aged and aged samples following ISO standard 37-2005 at room temperature. Tensile strength, stress at 100% elongation, and elongation at break were measured using U-CAN UT-2060 (Taiwan) instrument at room temperature with a speed of 500 mm/min. Shore A hardness was performed following ISO standard 7619-1986 using XY-1 sclerometer (Shanghai).

Acknowledgements

The authors would like to thank Nature Science sclerometer Foundation of China (50573021) and Groups Project of Guang Dong Province Nature Science Foundation (39172) for their financial supports.

References

- [1] Ray, S.S.; Yamada, K.; Okamoto, M.; Fujimoto, Y.; Ogami, A.; Ueda, K. *Polymer* **2003**, 44, 6633.
- [2] Arroyo, M.; López-Manchado, M.A.; Herrero, B. *Polymer* **2003**, 44, 2447.
- [3] Peeterbroeck, S.; Alexandre, M.; Je´ roˆ me, R.; Dubois, P. *Polym. Degrad. Stab.* **2005**, 90, 288.
- [4] Finnigan, B.; Martin, D.; Halley, P.; Truss, R.; Campbell, K. *J. Appl. Polym. Sci.* **2005**, 97, 300.
- [5] Krikorian, V.; Pochan, D.J. *Chem. Mater.* **2003**, 15, 4317.
- [6] Wang, Z.M.; Nakajima, H.; Manias, E.; Chung, T.C. *Macromolecules* **2003**, 36, 8919.
- [7] Viville, P.; Lazzaroni, R.; Pollet, E.; Alexandre, M.; Dubois, P. *J. Am. Chem. Soc.* **2004**, 126, 9007.

- [8] Ray, S.S.; Yamada, K.; Okamoto, M. *Macromolecules* **2003**, 36, 2355.
- [9] Chen, G.X.; Kim, H.S.; Shim, H.; Yoon, J.S. *Macromolecules* **2005**, 38, 3738.
- [10] Kawasumi, M. *J. Polym. Sci. Pol. Chem.* **2004**, 42, 819.
- [11] Wang, Y.Q.; Wu, Y.P.; Zhang, H.F.; Zhao, W.; Wang, C.X.; Zhang, L.Q. *Polymer* **2005**, 37, 154.
- [12] Gatos, K.G.; Sawanis, N.S.; Apostolov, A.A.; Thomann, R.; Karger-Kocsis, J. *Macromol. Mater. Eng.* **2004**, 289, 1079.
- [13] Herrmann, W.; Uhl, C.; Heinrich, G.; Jehnichen, D. *Polym. Bull.* **2006**, 57, 395.
- [14] Karger-Kocsis, J.; Wu, C. M. *Polym. Eng. Sci.* **2004**, 44:1083-1093.
- [15] Gatos, K. G.; Százdi, L.; Pukánszky, B.; Karger-Kocsis, J. *Macromol. Rapid Commun.* **2005**, 26, 915-919.
- [16] Kim, J. T.; Oh, T. S.; Lee, D. H. *Polym Int*, **2003**, 52, 1058.
- [17] Wu, Y. P.; Ma, Y.; Wang, Y.Q.; Zhang, L.Q. *Macromol. Mater. Eng.* **2004**, 289, 890.
- [18] Schon F, Thomann R, Gronski W. *Macromol.Symp.***2002**, 189, 105.
- [19] Kato, M.; Tsukigase, A.; Tanaka, H.; Usuki, A.; Inai, I. *J. Polym. Sci. Pol. Chem.* **2006**, 44, 1182.
- [20] Nah, C.W.; Ryu, H.J.; Kim, W.D.; Choi, S.S. *Polym. Advan. Technol.* **2002**, 13, 649.
- [21] Tidjani, A.; Wald, O.; Pohl, M.M.; Hentschel, M.P.; Schartel, B. *Polym. Degrad. Stab.* **2003**, 82, 133.
- [22] Cai, Y.B.; Hu, Y.; Song, L.; Lu, H.D.; Chen, Z.Y.; Fan, W.C. *Thermochim. Acta.* **2006**, 451, 44.
- [23] Yang, M.S.; Qin, H.L.; Zhang, S.M.; Zhao, C.G.; Hu, G.J. *Polymer* **2005**, 46, 8386
- [24] Vyazovkin, S.; Dranca, I.; Fan, X.W.; Advincula, R. *J. Phys. Chem. B.* **2004**, 108, 11672
- [25] Hashimoto, K. *Handbook of Elastomers*. New York: Marcel Dekker Inc., **1988**, 741.
- [26] Nakagawa, T. *J. Elastom. Plast.* **1992**, 24, 240.
- [27] Wrana, C.; Reinartz, K.; Winkelbach, H.R. *Macromol. Mater. Eng.* **2001**, 286, 657.
- [28] Chavarria, F.; Paul, D.R. *Polymer* **2006**, 47 (22), 7760.
- [29] Zilg, C.; Thomann, R.; Muelhaupt, R.; Finter, J. *Adv. Mater.* **1999**, 11, 49.
- [30] Kim, J.T.; Oh, T.S.; Lee, D.H. *Polym. Int.* **2003**, 52, 10583.
- [31] Liang, Y.R.; Lu, Y.L.; Wu, Y.P.; Ma, Y.; Zhang, L.Q. *Macromol. Rapid. Commun.* **2005**, 26, 926.
- [32] Chen. G. X.; Kim, E.S.; Yoon, J.S. *J. Appl. Polym. Sci.* **2005**, 98, 1727.
- [33] Thavamani, P.; Khastgir, D. *J. Elastom. Plast.* **1997**, 29, 124.
- [34] Li, F.X.; Xu, X.J.; Li, Q.B.; Li, Y.; Zhang, H.Y.; Yu, J.Y.; Cao, A.M. *Polym. Degrad. Stab.* **2006**, 91, 1685.
- [35] Park, J.W.; Oh, S.C.; Lee, H.P.; Kim, H.T.; Yoo, K.O. *Polym. Degrad. Stab.* **2000**, 67, 535.
- [36] Ozawa, T. *Bull. Chem. Soc. Jpn.* **1965**, 38, 1881.
- [37] Flynn, J.H.; Wall, L.A. *J. Polym. Sci. Part B. Polymer letter* **1966**, 4, 323.
- [38] Kissinger, H.E. *Anal. Chem.* **1957**, 29, 1702.
- [39] Zong, R.W.; Hu, Y.; Wang, S.F.; Song, L. *Polym. Degrad. Stab.* **2004**, 83, 423.
- [40] Leszczyńska, A.; Njuguna, J.; Pielichowski, K.; Banerjee, J.R. *Thermochim. Acta.* **2007**, 453, 75.
- [41] Leszczyńska, A.; Njuguna, J.; Pielichowski, K.; Banerjee, J.R. *Thermochim. Acta.* **2007**, 454, 1.